

LIMNOLOGY and OCEANOGRAPHY



Limnol. Oceanogr. 70, 2025, 3155–3171
© 2025 The Author(s). Limnology and Oceanography published by Wiley Periodicals LLC
on behalf of Association for the Sciences of Limnology and Oceanography.
doi: 10.1002/lno.70194

RESEARCH ARTICLE

Contact-dependent iron uptake from dust revealed by elemental analysis of single *Trichodesmium* colonies

Yeala Shaked [©], ^{1,2*} Futing Zhang [©], ^{1,2,3} Antonio Colussi [©], ^{4,5} Ana Esther Mijovilovich [©], ⁴ Meri Eichner [©], ³ Siyuan Wang [©], ^{1,2,a} Coco Koedooder [©], ^{1,2,6} Ondrej Prasil [©], ³ Syed Nadeem Hussain Bokhari [©], ⁴ Hendrik Küpper ^{©4,5*}

¹The Fredy and Nadine Herrmann Institute of Earth Sciences, Hebrew University of Jerusalem, Jerusalem, Israel; ²The Interuniversity Institute for Marine Sciences in Eilat, Eilat, Israel; ³Centre Algatech, Institute of Microbiology of the Czech Academy of Sciences, Třeboň, Czech Republic; ⁴Czech Academy of Sciences, Biology Centre, Institute of Plant Molecular Biology, Laboratory of Plant Biophysics & Biochemistry, České Budějovice, Czech Republic; ⁵Faculty of Science, University of South Bohemia, České Budějovice, Czech Republic; ⁶Israel Limnology and Oceanography Research, Haifa, Israel

Abstract

Aerosol dust deposited on the nutrient-deprived surface ocean can boost phytoplankton growth and oceanic carbon uptake. Low mineral solubility restricts the biological utilization of dust-nutrients, thereby benefiting phytoplankton that actively dissolve dust. The ubiquitous colony-forming, N₂-fixing cyanobacteria Trichodesmium specialize in dust-nutrient utilization, with several dust-dissolution pathways identified in natural populations. Studying active dust dissolution by Trichodesmium, we surveyed the elemental composition (i.e., quotas) of natural colonies from the dust-impacted Red Sea using a benchtop micro-x-ray fluorescence imager. We also examined changes in the colonies' quotas during incubations with dust and nutrients. Accounting for inter-colony variability, we analyzed 106 individual colonies. Since particles often appeared on the surface of colonies, we carefully analyzed all images, removing dust particle signals from colony quotas. Focusing on the colonies' iron (Fe) and phosphorus (P) quotas, we observed contrasting patterns of inter-colony variability and responses to dust, likely reflecting distinct nutrient sources—Fe sourced from dust and P sourced from the dissolved phase. Iron uptake from dust was repeatedly observed, but only upon colony-mineral interactions, indicative of contact-dependent active dissolution. The role of dust in Fe nutrition was also evident from the minor impact of dissolved Fe complexation on Fe quotas. Phosphorus quotas responded rapidly to P addition or removal, but not to dust. Natural colonies collected over a season had heterogeneous Fe quotas but homogeneous P quotas, further supporting their distinct sources. Predictions of Trichodesmium's bloom dynamics in particle-rich and dust-impacted ocean environments should incorporate its ability to dissolve Fe-minerals.

This is an open access article under the terms of the Creative Commons Attribution License, which permits use, distribution and reproduction in any medium, provided the original work is properly cited.

Associate editor: Susanne Wilken

Futing Zhang and Antonio Colussi equally contributed to this study.

Trichodesmium spp., a warm-water N₂-fixing cyanobacterium, is a keystone specie in tropical and sub-tropical ecosystems and plays an important role in ocean biogeochemistry (Luo et al. 2012; Tang and Cassar 2019; Tang et al. 2020; Benavides et al. 2021). Its ecological and biogeochemical importance is linked to its unique lifestyle, namely the formation of millimeter-sized colonies and extensive blooms at the ocean surface (Capone et al. 1997; Eichner et al. 2023; Qi et al. 2023). Trichodesmium fuels primary productivity and oceanic carbon uptake by introducing new N sources to nitrogendeprived seawater and thus supports energy and matter transfer through various food webs (Bergman et al. 2013;

^{*}Correspondence: yeala.shaked@mail.huji.ac.il; hendrik.kuepper@umbr.cas.cz

^aPresent address: School of Ocean Sciences, China University of Geosciences, Beijing, China

Berman-Frank et al. 2001; Pierella Karlusich et al. 2021). *Trichodesmium* may also contribute to carbon export, especially if its large blooms collapse and sink rapidly as large aggregates, often associated with ballasting dust particles (Bar-Zeev et al. 2013; Pabortsava et al. 2017; Bonnet et al. 2023). Several climate-change studies have predicted that the global distribution of *Trichodesmium* and N₂ fixation rates will further increase as temperatures and atmospheric CO₂ levels rise (Jiang et al. 2018; Walworth et al. 2018; Boatman et al. 2020). It was also referred to as a biodiversity hotspot, providing multiple microorganisms with physical support, shelter from grazing, a nest for reproduction, and a vessel for dispersion (O'Neil 1998; Zhang et al. 2024).

The basic unit of this filamentous cyanobacteria is the trichome, composed of tens to hundreds of cells. These trichomes can aggregate to form millimeter-sized colonies containing hundreds to thousands of trichomes (Capone et al. 1997). These colonies are composed of single or multiple species of Trichodesmium and exhibit varying sizes, shapes, and spatial arrangements, with the most common morphotypes being termed puffs and tufts (McCarthy and Carpenter 1979). In addition, these colonies host a diverse array of other microorganisms, including bacteria, phytoplankton, and even zooplankton (Sheridan et al. 2002; Koedooder et al. 2023). Colony formation entails both benefits and disadvantages for nutrient acquisition. The large colony size and its elevated nutrient demand can result in diffusion limitation for dissolved nutrient supply (Sommer et al. 2017), driving colonies to access other nutrient sources that are typically unavailable to phytoplankton (Eichner et al. 2023). Such sources include minerals and particles (Rubin et al. 2011; Polyviou et al. 2018) and a range of organic molecules (Van Mooy et al. 2012; Frischkorn et al. 2018). The features that aid colonies in diversifying their nutrient sources involve the excretion of hydrolytic enzymes and metal-binding molecules, often orchestrated by bacteria cohabiting the colonies (Basu et al. 2019; Frischkorn et al. 2017; Gledhill et al. 2019; Koedooder et al. 2023).

In many oligotrophic environments, *Trichodesmium* is subjected to iron (Fe) and phosphorus (P) limitation or colimitation (Paerl et al. 1994; Sañudo-Wilhelmy et al. 2001; Webb et al. 2007; Held et al. 2020; Cerdan-Garcia et al. 2022). *Trichodesmium* acclimates to Fe-limitation by down-regulation of N₂-fixation and adjustment of photosynthetic electron flow (Küpper et al. 2008; Colussi et al. 2024). Deposition of aerosols such as desert dust or ash on the ocean surface can sporadically alleviate this nutrient stress and support *Trichodesmium* blooms (Chen et al. 2011; Lenes et al. 2008). Multiple culture experiments, on-deck incubation, and remote-sensing observations established the importance of desert dust and additional aerosols for *Trichodesmium*'s growth and N₂-fixation (Mills et al. 2004; Langlois et al. 2012; Benavides et al. 2013).

In addition, mechanistic studies have revealed that a range of adaptations for dust utilization exists in natural Trichodesmium colonies. The colonies can prevent dust loss due to sinking by efficiently capturing and redistributing dust to their cores (Rubin et al. 2011; Kessler et al. 2020a; Wang, et al. 2022a). Since the solubility of dust minerals is often low and dissolution is a prerequisite for uptake, recent studies focus on colony-mediated pathways for active dust dissolution, such as reductive and ligand-promoted dissolution (Basu and Shaked 2018; Eichner et al. 2019, 2020; Shaked et al., 2023). A noteworthy recent finding is the mutualistic interactions of Trichodesmium with its associated bacteria that synthesize mineral-solubilizing compounds (siderophores), some of which are photolabile and thus can distribute the dissolved Fe to the entire consortium (Basu et al. 2019; Koedooder et al. 2023). Further evidence for active colony-mediated dust dissolution comes from the upregulation of unique genes and proteins upon physical interaction of colonies with dust (Polyviou et al. 2018; Held et al. 2021).

Such a capability of actively dissolving the almost insoluble dust minerals can provide Trichodesmium a competitive advantage over other phytoplankton (Basu et al. 2019). Upon its demise, Trichodesmium may further fertilize the ocean with these nutrients (Shaked et al. 2024). A common method for probing active mineral dissolution involves comparing uptake with and without cell-mineral contact, where contact is prevented by placing the mineral in a dialysis bag (Kranzler et al. 2016). However, the presence of minerals on cells, which are difficult to remove, complicates these uptake measurements. Subsequently, these particles add to the overall cell signal and prevent the quantification of intracellular elemental concentrations or quotas. Elemental imaging with a micro x-ray fluorescence (μ XRF) imager offers a way to overcome this challenge. Given the high spatial resolution of images obtained by μ XRF, areas of interest, such as dust, can be separated from the cells (van der Ent et al. 2018). This process of image analysis is termed masking and has also been established for benchtop systems in 2D mode (Mijovilovich et al. 2020).

Here, seeking to explore nutrient uptake from dust by *Trichodesmium* and, specifically, its ability to dissolve dust actively, we examined the elemental composition of individual natural colonies from the dust-impacted Red Sea. Utilizing our highly accessible, in-house, customized benchtop μ XRF imager, we analyzed 106 individual colonies from multiple morphotypes and species. By combining in situ collection of colonies and incubation experiments, we probed for changes in colony composition in response to dust and nutrient addition (or removal). Since particles were often associated with the colonies, we had to mask them by performing a detailed image analysis. Through image analysis, we also examined the spatial distribution of elements between the colony core and its periphery. We then analyzed this rich dataset, focusing on the iron and phosphorus content (quotas) of the colonies.

are governed by the applicable Creative Commons

Collectively, our findings suggest that Red Sea *Trichodesmium* colonies obtain phosphorus from the dissolved phase, while iron is acquired from the particulate phase through contact-dependent active dissolution of dust.

Methods

Colony collection and preparation for µXRF analysis

We collected natural *Trichodesmium* spp. colonies from the northern Gulf of Aqaba during the spring and autumn of 2021 (29.56°N, 34.95°E). Colony density was elevated in these periods (0.1–4 colonies per cubic meter), but no surface blooms were recorded. In spring, different puff-shaped colony morphotypes of *Trichodesmium thiebautii* (Koedooder et al. 2022) were prepared for analysis immediately upon collection to examine in situ changes in elemental composition (Table 1; Supporting Information Section 1). In autumn, colonies were incubated for up to 8 d under semi-natural conditions to track their nutrient uptake dynamics and investigate active contact-dependent dust dissolution.

We collected the colonies offshore from 10 to 20 m depths using a 100 µm phytoplankton net towed from a motor boat at slow speed (0.5 knots). We immediately diluted the net concentrate into $\sim 10\,L$ surface seawater to alleviate stress. In the lab, we handpicked the colonies using Pasteur pipettes or plastic droppers and suspended them in Petri dishes containing 0.22 µm sterile-filtered fresh seawater (FSW). We separated different colony morphotypes and washed them thrice by transferring them into new Petri dishes with FSW under a stereoscope. We then distributed the washed colonies, one by one, on acid-washed polycarbonate filter membranes (5 µm pore size). Excess seawater was adsorbed by a tissue paper placed beneath the filter membrane to minimize NaCl precipitation on the filaments. We put the filter in an acidcleaned Petri dish to avoid contamination with dust and particles and quickly dipped it into liquid nitrogen. Prior to transfer to the μXRF , all frozen filters were further freeze-dried.

Incubation experiments

Incubations were performed in autumn 2021, probing for the effect of changing nutrient fluxes and dust addition on the colony elemental composition. Colonies were collected and treated as explained above and then suspended for incubations in 125 mL acid-cleaned Nalgene bottles filled with FSW. The bottles were hung under the Interuniversity Institute for Marine Sciences pier at 1–2 m depth. This allowed colonies to maintain their circadian cycle and remain at ambient temperature with some turbulence. These conditions were carefully chosen following multiple unsuccessful trials to keep natural *Trichodesmium* colonies intact for longer than a day.

Four different incubations, varying in length and treatments, were designed to capture the time window and conditions that yield measurable changes in intracellular elemental composition (quota). The 1st incubation lasted 2 d and included four treatments: FSW, +P (10 µM KH₂PO₄), and +dust (2 mg L^{-1}) added within a dialysis bag (to prevent contact with the colonies) or in suspension. This incubation was sampled after 24 and 48 h (Table 1). The 2nd week-long incubation included two treatments: FSW and deferoxamine B (DFB, $1 \mu M$), a strong Fe chelator that, when added in excess, was shown to diminish Fe uptake (Rubin et al. 2011). The 3rd experiment included a week-long incubation in FSW or DFB to induce P/Fe-limitation, followed by a day-long incubation with dust (2 mg L^{-1}) (Table 1). In the 4th incubation, tuftshaped Trichodesmium erythraeum colonies were maintained for a week in FSW, +P (10 μ M KH₂PO₄), and P + DFB (10 μ M, $1 \mu M$, respectively). The physiological state of the colonies, indicated by the colony form, color, and position in the bottle, was examined daily.

Table 1. An overview of the study, detailing collection periods, *Trichodesmium* species and morphotypes, number of analyzed colonies, and incubation duration and treatments.

Date	Data type	Species and morphotypes	Colony #	Treatment					
				FSW	DFB	P	Dust		Duration
							Suspension	Dialysis bag	
Autumn 2021	Incubation #1	Trichodesmium thiebautii puffs	30	V	V	V	V	V	2
	Incubation #2	T. thiebautii puffs	10	V	V				7
	Incubation #3	T. thiebautii puffs	20	V	V		V		8
	Incubation #4	Trichodesmium erythraeum tufts	20	V	V	٧	V		7
Spring 2021	In situ	T. thiebautii thin puffs	11	V*					0
		T. thiebautii dense puffs	9	V*					0
		T. thiebautii amoebae-containing puffs	7	V *					0

^{*}Colonies were washed three times in filtered seawater (FSW) before freezing.

Shaked et al.

Dust collection and characterization

Desert dust was collected at the northern Gulf of Aqaba at the Interuniversity Institute of Marine Sciences in Eilat. Israel. This dust originates from the Sahara and the Arabian Peninsula, and it is considered a significant source of mineral particles to the surface water of the Gulf (Torfstein et al. 2017). A bulk dust sample was collected over several weeks using a static plastic, polyvinyl chloride aerosol collector, positioned horizontally to facilitate settling. It was sieved through a 200 μ m mesh to remove fibers and large particles, and then stored in a desiccator (Visser et al. 2025). The primary minerals in the dust were silicates (quartz and aluminosilicates), accounting for half of the dust mass, followed by carbonates ($\sim 40\%$) and evaporites (10%). The dust's total Fe content estimated by extraction was 3.5% (~ 600 μ mole Fe g⁻¹ dust), while its total P content was only 0.1– 0.2% (40–70 μ mole P g⁻¹ dust) (Kessler et al. 2020a, 2020b).

Elemental analysis in benchtop μXRF *Instrument*

X-ray fluorescence images were collected at 16 μm resolution (beam size), $4\times$ oversampling (4 $\mu m)$ and 750–1100 ms

integration time per pixel with a customized benchtop μ XRF BRUKER M4 TORNADO (Bruker Nano GmbH) as described in (Mijovilovich et al. 2020) and the Supporting Information. Polycarbonate filters with freeze-dried colonies (see above) were mounted on top of an acid-washed hollow 10-cm side cubic polycarbonate box to reduce photon scattering, with a printer foil supporting the membrane (details in Colussi et al. 2024).

Image analysis

Elemental images were analyzed, separating the background from the colony, selecting different colony regions, and masking abiotic particles. Automatic selection was not possible due to the colonies' low signals. The colony's borders were drawn manually using ImageJ/Fiji on the pictures taken from a stereomicroscope before the μ XRF analysis (Fig. 1). These contours were then applied to the elemental maps (mainly Cl and/or K maps, due to a higher signal/background ratio) and rotated/resized to fit these lower-resolution images. Dust particles were selected from the elemental images based on their round regular shape, their high signal that was far exceeding that of the biological material, and their "unique" elemental composition that

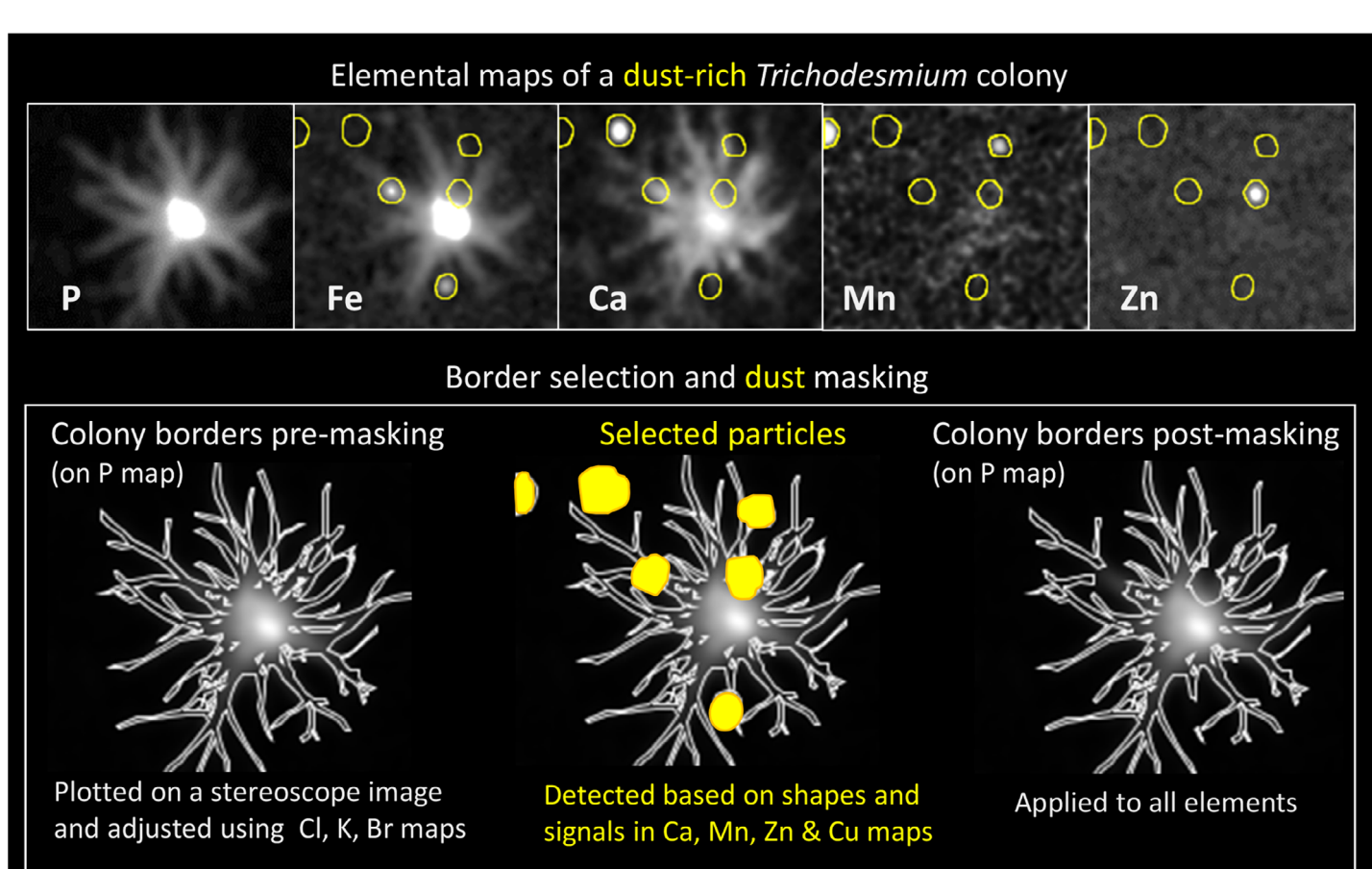


Fig. 1. Schematic representation of the image analysis procedure we conducted on all 106 *Trichodesmium* colonies analyzed by micro-x-ray fluorescence (μXRF). Several elemental maps of a dust-rich puff-shaped *Trichodesmium thiebautii* colony are shown in the upper panel, based on which we identified the dust particles. On the lower panel, we demonstrate the colony border selection and the masking of dust particles.

Shaked et al.

made them visible in only a few elemental maps (mainly Ni, Zn, Fe, Mn, e.g., Fig. 1). Unlike light microscopy, μ XRF can detect particles smaller than the instrument beam size (16 μ m), as long as their concentrations exceed the detection limit, as is often the case for Fe-rich particles. The signals from these particles were then subtracted from the regions belonging to the colony. Average areal counts (or concentrations) were calculated by image analysis software (ImageJ/Fiji) for the entire colony and selected regions (Supporting Information Section 3.5).

Calibration with a thin reference

Since the colonies are much thinner than typical XRF calibration foils ($\sim 10~\mu m$ vs. 200–400 μm), we prepared two sets of very slim references from a certified soybean standard and laboratory-grown *Trichodesmium*. Standard preparation and calibration procedures are described in detail in the Supporting Information (Section 3.2). The *Trichodesmium* reference was quantified in both XRF and inductively coupled plasma mass spectrometer (ICP-MS), yielding comparable Fe/P ratios; therefore, validating the calibration with the thin soybean reference (Supporting Information Table S2). Based on the soybean reference, Ca, Fe, and P were converted from counts per second to ppm. Chlorine and nickel were not detectable in the soybean reference, and their response factors were calculated theoretically (Supporting Information Section 3.3).

Quantification and normalization

Due to the overlap of the trichomes in the colonies, their biomass cannot be determined properly. We addressed this issue by dividing the element of interest by an element with a relatively

homogeneous distribution that would mimic the biomass to achieve a "biomass normalization". We find that the ubiquitous and intense chlorine (Cl) signal can be used to account for the biomass, despite also being a major constituent of seawater. In our μ XRF maps of freeze-dried samples, we observed that Cl forms a thin layer on the trichomes, with a linear dependence on the number of overlapping trichomes, as detailed in the Supporting Information (Section 3.4). However, since the choice of the normalizer element is not trivial, we also normalized against additional elements, such as S, K, and Ca, to compare the results.

Results

Overview

In this study, we utilized a benchtop μ XRF to probe whether natural *Trichodesmium* colonies can actively mine dust for nutrients through contact-dependent dust dissolution. We conducted our study in the dust-impacted Red Sea, combining in situ colony collection and semi-controlled incubation experiments (Table 1). Through multiple iterations, we streamlined our sampling and incubation strategies, sample preparation, and analytical procedures, obtaining multiple elemental maps for 106 individual colonies. We carefully analyzed these images to mask dust particles, thereby quantifying the chemical composition of the colonies and the spatial distribution of elements between the colony core and periphery.

Elemental maps and dataset characteristics

In Fig. 2, we show μ XRF images from the most common morphotypes and treatments. The best-detected elements,

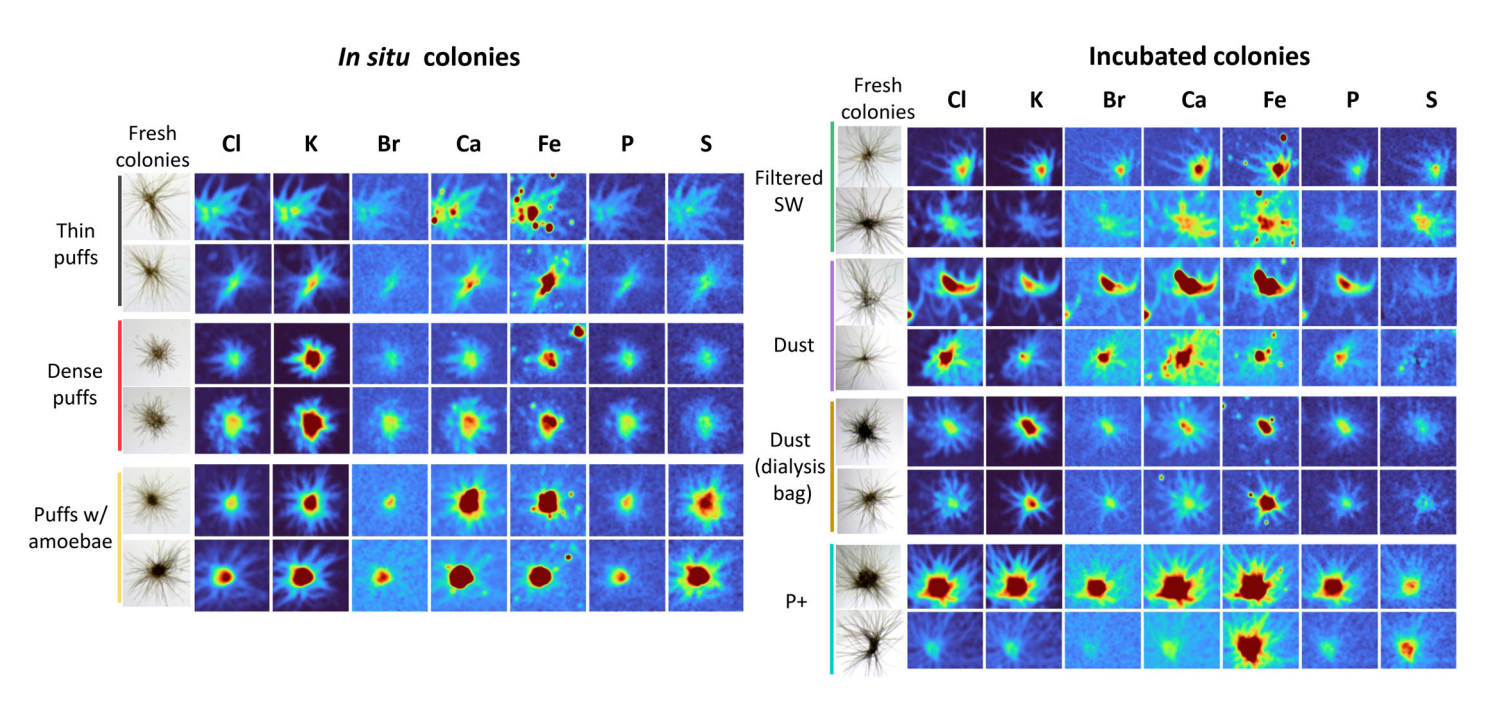


Fig. 2. Images and micro-x-ray fluorescence (μXRF) elemental maps of the common Red Sea *Trichodesmium thiebautii* morphotypes freshly collected (i.e., in situ) or incubated with dust and nutrients for up to a week (i.e., incubations). Many images contain Fe and Ca-rich dust particles that were masked before calculating the elemental composition of the colony (*see* "Methods" section).

which generated clear maps of the entire colony, were chlorine (Cl), potassium (K), bromine (Br), iron (Fe), arsenic (As), and phosphorus (P). Calcium (Ca) and sulfur (S) had lower signal-to-background ratios but were still mapped along the colony shape (Fig. 2; Supporting Information Fig. S6). Additional elements, including copper (Cu), manganese (Mn), zinc (Zn), and nickel (Ni), were visible only in some colony cores (Supporting Information Fig. S6). Compared to a synchrotron beamline with a tunable monochromatic light source, benchtop μ XRF using a Rh tube has lower sensitivity, particularly for light elements. Still, its relative accessibility enabled us to obtain a considerable sample size of 106 Trichodesmium colonies, for which it would be very unlikely to receive sufficient synchrotron beam time. This rich dataset provides insights into the elemental composition and distribution of single Trichodesmium colonies, as well as their response to external nutrient fluxes.

The selected sample preparation with initial freezing in liquid nitrogen, followed by freeze drying, resulted in good preservation of the intricate colony structure (Fig. 2). It also prevented the redistribution of dissolved elements, unavoidable when using chemical fixation, and hence our sample preparation enabled rigorous comparison of colonies analyzed over 2 years. This is especially true for elements that tend to leak from cells, with K being the most easily lost, as it forms no covalent bonds and only weak complexes (van der Ent et al. 2018).

Due to the two-dimensional nature of the μ XRF method, obtaining absolute elemental concentrations of colonies with overlapping trichomes is hard. Nonetheless, the μ XRF method offers invaluable advantages for inter-colony comparisons, which are key for understanding their response to the dynamic nutrient regimes in the ocean and our incubations. As shown clearly by the images in Fig. 2, Trichodesmium colonies differed markedly in size, filament arrangement, and filament number, which complicates the comparison among colonies. Here, however, we could obtain accurate inter-colony comparisons by using elemental ratios, with the denominator element serving to normalize for biomass. Image-based analytical techniques often utilize elemental ratios to correct for steric effects, size, or biomass differences (Nuester et al. 2012); hence, the data we present next are expressed as elemental ratios rather than concentrations or counts.

Most of the colonies contained particles that could skew the quantification of their elemental composition (Fig. 2). However, these particles are easily recognized by their distinct shapes and high signals compared to those of the colony (e.g., very high Ni, Zn, Fe, Mn, and Ca). Such particles were carefully examined in different elemental maps, selected, and excluded from the whole colony elemental signal or concentration (Fig. 1; Supporting Information Section 3.5).

Spatial distribution within colonies

We examined the spatial distribution of elements within colonies by sectioning the colony images into core and periphery zones. Accounting for biomass differences, we calculated elemental ratios and divided the elemental ratios of the core by those of the periphery. This way, elements enriched in the colony core appear as > 1, while elements depleted in the colony core appear as < 1 (Fig. 3). We performed the analysis on colonies from all treatments using multiple elements in the denominator (Cl, Br, K, S). We excluded elongated tufts and amoebae-containing colonies from the analysis. The observed patterns were shared by most colonies, regardless of their incubation treatment, and were denominator-independent (Fig. 3). Calcium was evenly distributed throughout the colony, yielding core/ periphery ratios close to 1. As, probably in the form of arsenate, was somewhat depleted in the colony center (20% depletion). Iron was strongly enriched (50-80%) in the colony center, and so were Ni and Mn (Supporting Information Table S3; Fig. S7). The degree of center enrichment varied among colonies, but it persisted in 80-90% of the tested colonies. Phosphorus was also enriched in the core, but to a lesser degree and not in all colonies (Fig. 3; Supporting Information Table S3). Regardless of their biological implications, analytically, the even distribution of calcium, a major dust component, supports the robustness of the dust masking approach.

Composition of different morphotypes and species

Our dataset included in situ collected T. thiebautii puffs (thin, dense, and amoebae-containing morphotypes), incubated T. thiebautii puffs (normal morphotype), and T. erythraeum tufts (Table 1; Fig. 2). Excluding nutrient-amended colonies, this dataset consists of \sim 50 colonies. Comparing many different elemental ratios (e.g., Fe/P, Mn/Cl, Ca/K), we found a relatively homogeneous composition among colonies of different morphotypes and species (Supporting Information Figs. S8, S9).

Amoebae-containing colonies appeared as notable exceptions, displaying elevated Ca and S and depleted As in the colony core where the associated amoebae were located. These visible patterns (Fig. 2) were also reflected in elemental ratios using multiple elements in the denominator (Cl, Br, K). These changes are likely attributed to the distinct elemental composition of the associated amoebae compared to Trichodesmium cells. Our recent study identified these amoebae as belonging to the genus Trichosphaerium (30 µm in diameter), characterized by a calcified shell, and further observed that a single colony can harbor over 40 such amoebae (Zhang et al. 2024). Since we did not mask the amoebae, their presence at high densities in some colonies strongly impacted their elemental composition. Colonies containing fewer amoebae had a similar composition as other amoebae-free colonies. Several distinct features of specific colony types, such as elevated Zn in thin colonies and depleted As in tufts, were also identified (Fig. 2; Supporting Information Figs. S8, S9).

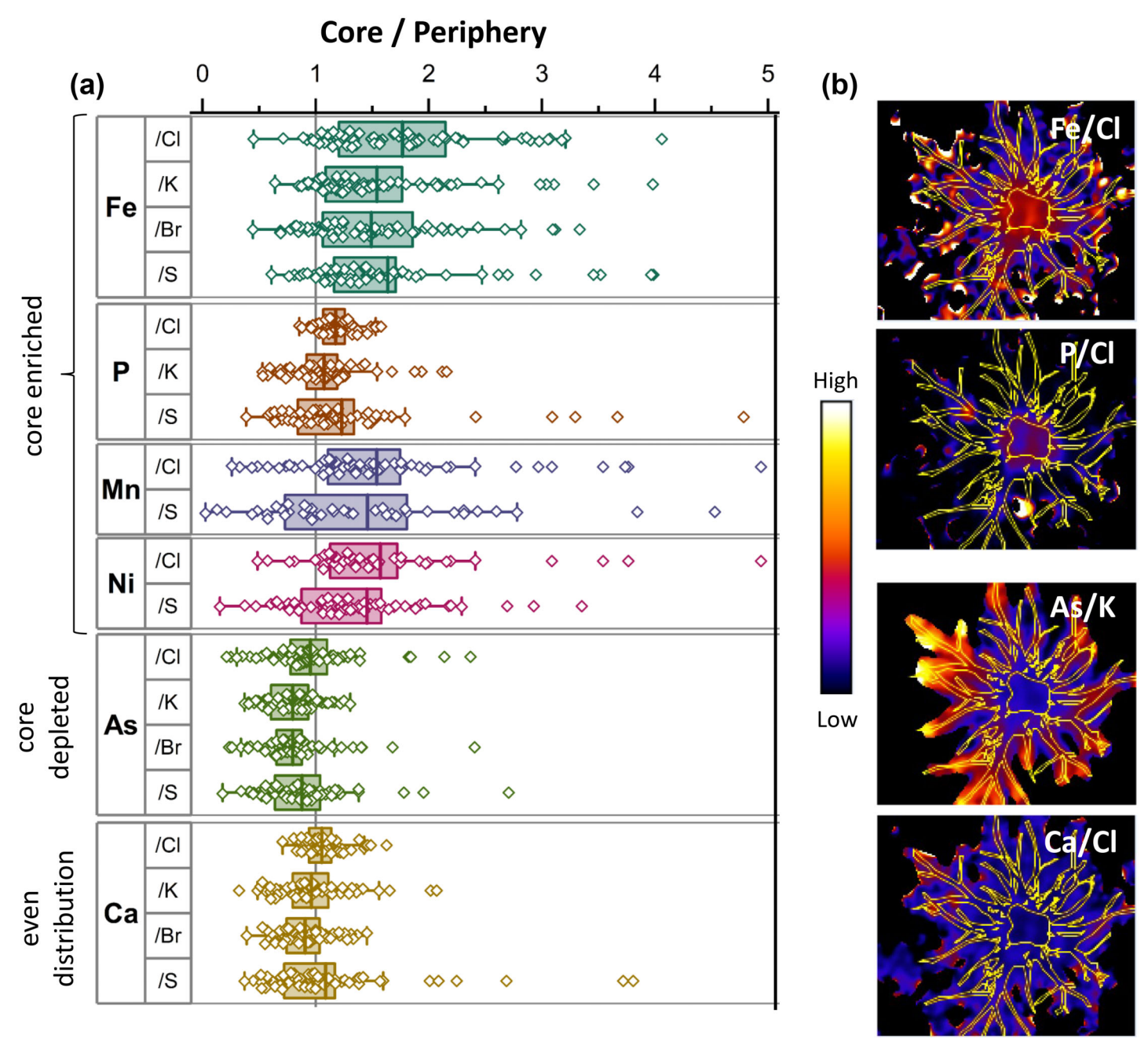


Fig. 3. The spatial distribution of elements within colonies presented as: (a) Elemental ratios of the core/periphery from the entire dataset, and (b) Elemental ratio maps of a representative colony. In both panels, we utilized several elements (CI, K, Br, S) as biomass normalizers to account for differences in biomass between the core and periphery. In (a), we further divided the element ratios of the core by those of the periphery, to facilitate comparison between the regions. As a result, core-enriched elements appear as > 1, core-depleted elements as < 1, and evenly distributed elements as 1. In (b), we show a relative color scale (as values differ between elemental ratios).

Effect of dust and nutrient addition on colony Fe quotas

Due to the complex colony structure with overlapping trichomes, whole colony Fe quotas can only be expressed as elemental ratios. Previous XRF-based studies of *Trichodesmium* utilized P and S as biomass normalizers (Nuester et al. 2012, 2014). Given our interest in P and sulfur's relatively low signal-to-background ratio, we chose Cl as a biomass

normalizer (*see* Supporting Information regarding NaCl precipitation). Having excluded the Fe signal of dust particles through image analysis, the Fe/Cl ratios reflect the colony Fe composition, referred to as Fe quota.

We examined changes in the Fe quota (Fe/Cl ratio) for the entire dataset, which comprises ~ 100 colonies (excluding colonies containing amoebae). In situ colonies had comparable

Shaked et al.

Fe quotas across morphologies, which also matched the incubation control (Fig. 4). Iron quotas did not decrease during 24-and 48-h incubations in FSW and remained unchanged even during 7- and 8-d incubations (Fig. 4, FSW). Incubations with DFB, added in excess to induce Fe-limitation by complexing the dissolved Fe and making it less available for uptake by the colonies (Lis and Shaked 2009), had only a minor impact. Iron quotas, expressed as Fe/Cl, remained unchanged during incubations with DFB (Fig. 4a, DFB), but when expressed as Fe/S, a slight drop was observed (Fig. 4b, DFB). The addition of dust in suspension, allowing interactions with the colonies, markedly increased the Fe quota. The response to dust was highly variable, with some colonies only doubling their Fe quotas, while others increased them by 10–20 fold (Fig. 4, Dust).

In contrast, Fe quotas of colonies incubated with dust placed in a dialysis bag remained unchanged (Fig. 4, [Dust]). Dust concentrations were similar in both treatments (2 mg L $^{-1}$), but the dialysis bag prevented interactions between the colony and the dust minerals. These data, thus, clearly show that cell-mineral contact is key to Fe uptake from dust. Overall, we observed similar trends when using S or Ca as biomass normalizers (Fig. 4b), except for the incubations with DFB. Intriguingly, colonies incubated with PO_4^{3-} markedly increased their Fe quota (Fig. 4, P). The increase in Fe quota due to PO_4^{3-} addition varied among colonies, possibly due to differences in incubation conditions or the initial nutrient status of the colonies.

Effect of dust and nutrient addition on colony P quotas

Next, we explore the colonies' P quotas expressed as P/Cl ratios for the same set of ~ 100 in situ and incubated colonies.

We first examine the short incubation #1 (November 23–24), which was sampled after 1 and 2 d and could thus inform the timing of changes in P quotas. In most treatments, P quotas changed markedly between the 1st and 2nd day, indicative of a rapid response to nutrient addition or removal (Fig. 5a). The colony's P quotas dropped between days when incubated in FSW (Fig. 5a), probably due to a depletion of P supply in the seawater. P quotas significantly increased with phosphate addition (10 μ M), with up to a three-fold increase (Fig. 5a, P). The change in the P quotas was gradual and became more pronounced by the 2nd day. The P quotas remained unchanged in incubations with suspended dust (Fig. 5a, Dust). Dust added within a dialysis bag slightly increased P quotas (Fig. 5a, [Dust]). This finding remains enigmatic since we analyzed this treatment only on the 1st day.

Finally, we combined all incubations to gain a broader understanding of the P quota dynamics (Fig. 5b). We observed similar patterns in the combined dataset, with a marked increase in P quotas following P addition (Fig. 5b, P). The lowest P quotas occurred in incubations with FSW (Fig. 5b). These quotas were comparable among short and long incubations and lower than those of in situ colonies. Dust and the Fechelator DFB did not affect P quotas (Fig. 5b, Dust, DFB).

Inter-colony variability in P and Fe quota

Lastly, we query this large dataset for inter-colony variability in Fe and P quotas and compare it to other single-colony measures. We examine the inter-colony variation in P quotas by calculating the coefficient of variation (CV) for each treatment (calculated as standard deviation/mean, 0.13–0.35;

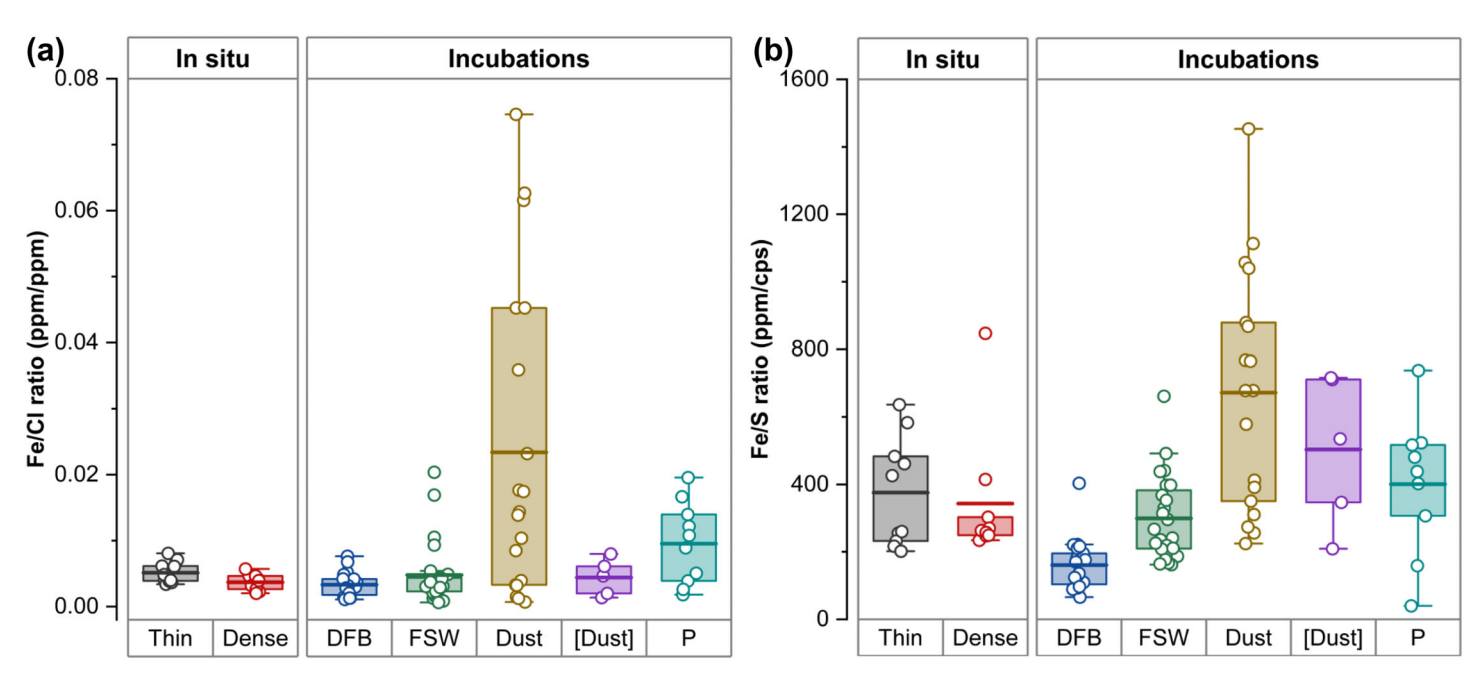


Fig. 4. Iron quotas of \sim 100 Red Sea *Trichodesmium* colonies freshly collected (in situ) or incubated for up to a week in filtered seawater (FSW) and with additions of a strong Fe-chelator (deferoxamine B, DFB), dust in suspension (Dust) or in a dialysis bag ([Dust]), and phosphate (P). The colony Fe quotas are expressed as ratios, using Cl (a) and S (b) as biomass normalizers.

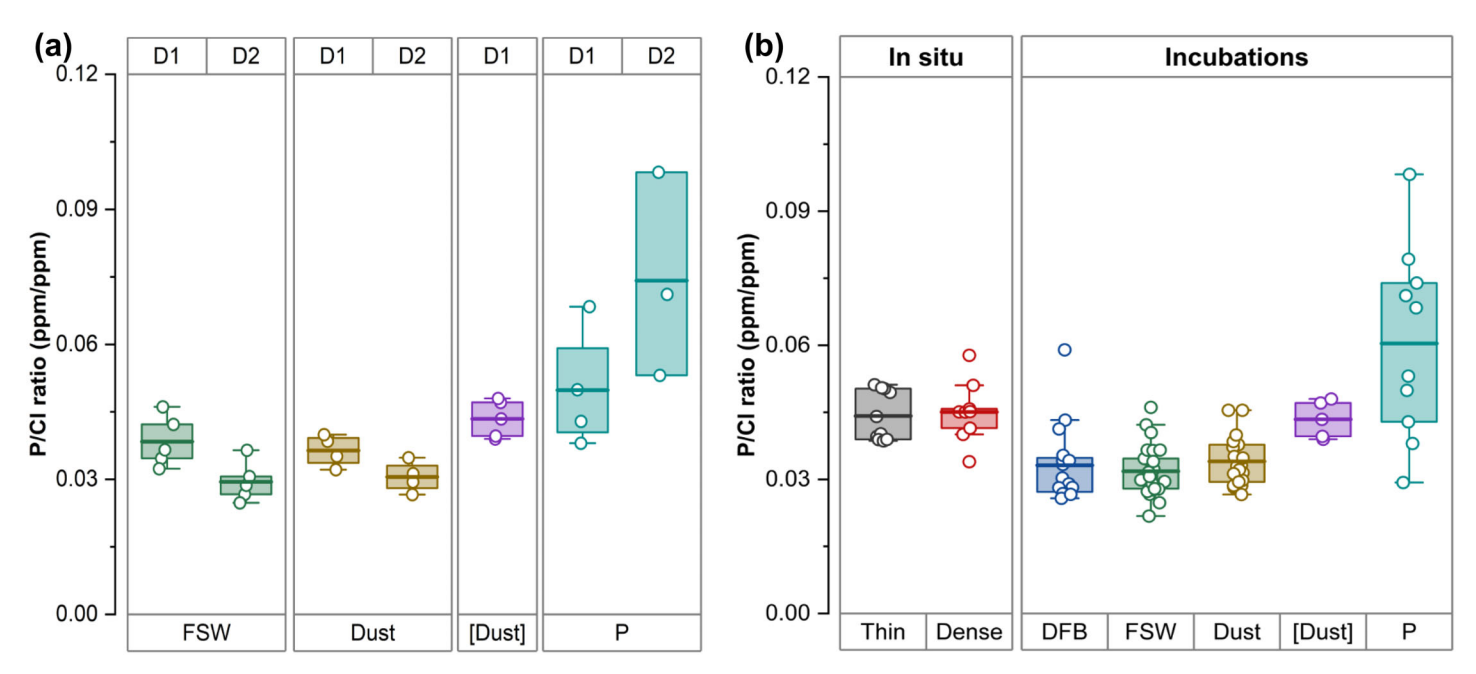


Fig. 5. Phosphorus quotas of \sim 100 Red Sea *Trichodesmium* colonies freshly collected (in situ) or incubated for up to a week with nutrients and dust. The colony P quotas are expressed as P/Cl. (a) Colonies collected after 1 d (D1) and 2 d (D2) of incubation # 1 (November 23–24, *see* Table 1) show rapid changes in their P quotas. Treatments include filtered seawater (FSW), dust in suspension (Dust) or in a dialysis bag ([Dust]), and phosphate (P). (b) Summary of P quotas of colonies from all four incubations, with treatments as described in Fig. 4 and Table 1.

Supporting Information Table S4). The same analysis for Fe quotas yielded a higher coefficient of variation (0.3–1; Supporting Information Table S4). We further visualize this scatter by normalizing the quotas by the maximal value of each treatment, yielding a 0–1 scale, where homogenous values cluster closer to 1 (Fig. 6). The homogeneity in P quotas is apparent from the high ratios shown in Fig. 6b, which are typically above 0.6 (i.e., less than 1.5-fold change from the maximal quota in each set). In contrast, Fe quotas are heterogeneous, with 40% of the values below 0.3 (i.e., above 3-fold change from the maximal quota in each set, Fig. 6a).

To further contextualize this finding, we compared the scatter in P quotas with that of single-colony alkaline phosphatase activity (APA), measured in the same spring season of 2021. These APA measurements were obtained weekly on ~ 10 freshly collected colonies, as described by Wang (2023). Phosphorus limitation by phytoplankton cells is commonly assessed through APA, which is regulated by their intercellular P concentrations (Stihl et al. 2001; Shaked et al. 2006; Dyhrman 2016). Indeed, high APA was frequently detected in Trichodesmium filaments and colonies from many ocean regions (including the Gulf of Aqaba) and was linked to P-stress or P-limitation (Dyhrman et al. 2002; Van Mooy et al. 2012). Here, we focus on intercolony variability in APA, which yielded a high coefficient of variation (0.32–0.96; Supporting Information Table S4). We also visualized the heterogeneity in APA using the same approach applied to the quotas. The resulting ratios, shown in Fig. 6c, were highly scattered and typically lower than

0.5. Plotting these two related P features in Fig. 6 further highlighted the homogeneity of P quotas in contrast to the heterogeneity of APA. These patterns may reflect the different time scales of these two parameters: APA represents real-time activity, while P quota represents a relatively long-term accumulation.

Discussion

Summary and overview

Previous studies using ICP-MS and synchrotron XRF have quantified the elemental composition of natural Trichodesmium colonies (Berman-Frank et al. 2001; Sañudo-Wilhelmy et al. 2001; Tovar-Sanchez et al. 2006; Chen et al. 2011; Nuester et al. 2012, 2014). Rather than reproducing these studies, we aimed here to characterize the compositional heterogeneity of natural colonies in the dust-impacted Red Sea environment and their response to external nutrient fluxes and dust availability. Expecting considerable heterogeneity in composition among colonies differing in morphology, size, filament numbers, and life history, we selected a benchtop μXRF as a balance between sensitivity and accessibility (Supporting Information Table S1). Another key goal of this research was to track Trichodesmium's ability to dissolve dust by following intracellular nutrient uptake. To achieve this goal, we had to account for the presence of dust on the colonies that can skew their intracellular composition (quotas). By analyzing μXRF images of multiple elements, we identified the dust particles and masked them from the colony quotas. We center our

19395590, 2025

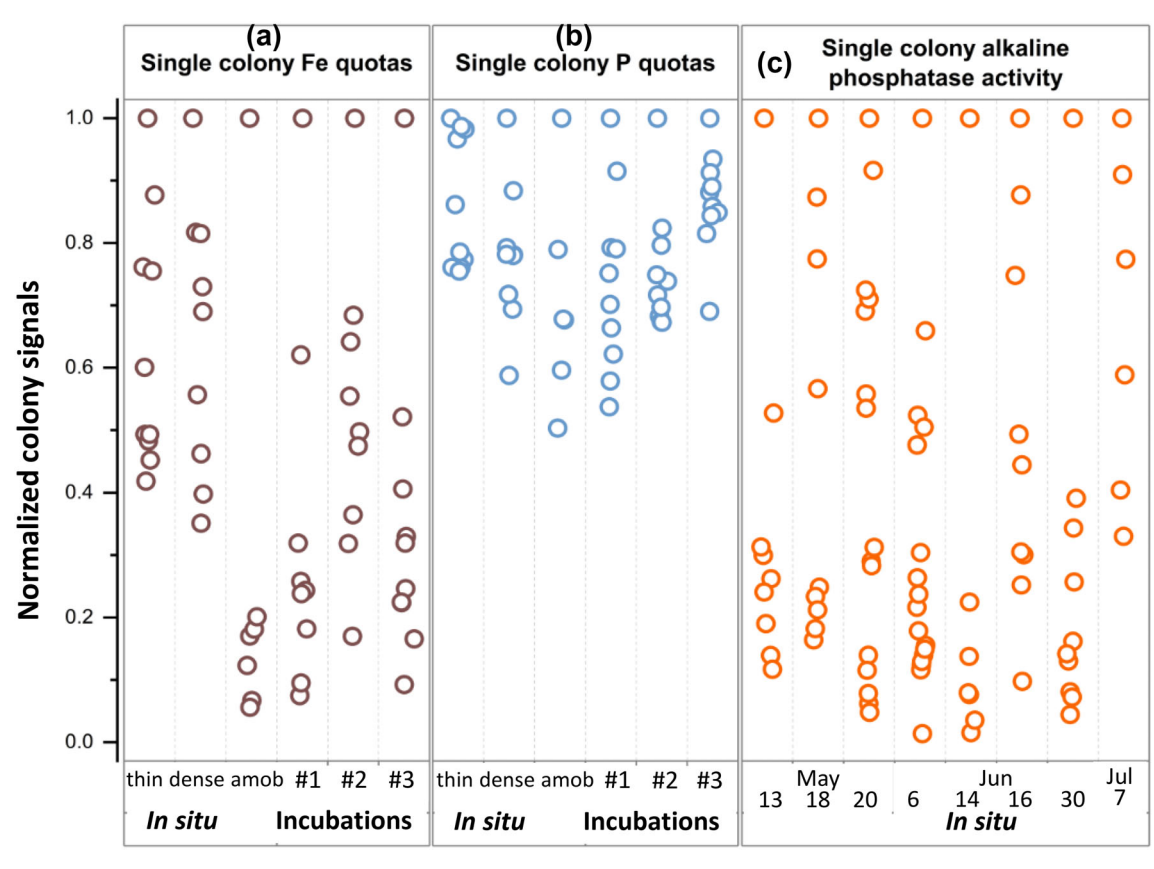


Fig. 6. Visualization of inter-colony variability obtained for single colony measurements of (a) iron quotas, (b) phosphorus quotas, and (c) alkaline phosphatase activity. To facilitate comparison between these datasets, values collected in each treatment or day were normalized to the highest value in this set, resulting in a 0–1 scale. Single colony measures closer to one represent homogeneity, whereas values closer to zero represent heterogeneity.

discussion on the key nutrients Fe and P, for which we obtained high μ XRF signals. To facilitate the discussion, we provide a graphical summary of our main findings in Fig. 7.

Contact-dependent iron uptake from dust

One of the significant findings of this study is the marked increase in Fe quotas (expressed as Fe/Cl or Fe/S) upon colony–dust contact (Fig. 4). This increase, indicative of Fe uptake, occurred in incubations where we observed interactions between colonies and dust. The contact-dependent Fe uptake from dust was highly variable, with some colonies barely increasing their Fe quotas while others reached up to a 30-fold increase. These inter-colony variations in Fe uptake highlight the stochastic nature of dust as an iron source for *Trichodesmium*. In contrast, Fe quotas remained unchanged when we prevented colony–dust interactions by placing the dust in a dialysis bag. The lack of Fe uptake in the dialysis bag incubations is expected, given the low solubility of this dust (Kessler et al. 2020b).

Our findings on the essential role of cell–dust contact for Fe acquisition from dust align with those of Rubin et al. (2011), who reported that the physical separation of synthetic radio-labeled ferrihydrite from *Trichodesmium* colonies

prevented Fe uptake. It also aligns with studies on natural or cultured Trichodesmium, which show differential gene expression or protein synthesis upon cell-dust contact (Held et al. 2021; Langlois et al. 2012; Polyviou et al. 2018). Several pathways have been proposed to facilitate the dissolution of Fe minerals by *Trichodesmium*, including reductive dissolution, siderophore-mediated dissolution, and superoxide-mediated dissolution (Rubin et al. 2011; Basu and Shaked 2018; Kessler et al. 2020b; Shaked et al., 2023, 2024; Romanowicz et al. 2024). Some of these pathways involve soluble reactants (Hansel et al. 2016; Gledhill et al. 2019), while others are contact-dependent, involving membrane-bound enzymes or short-range electron transfer (Gralnick and Newman 2007). Regardless of the employed pathways, the physical confinement of the dust among the many trichomes in the colony core is key to both dissolution and uptake, as it minimizes diffusion distances of dissolved Fe to the cell surface and thus reduces diffusive losses (Basu and Shaked 2018; Basu et al. 2019; Eichner et al. 2020).

Phosphorus nutrition and dynamics

In contrast to Fe, the colony's P quotas did not increase after dust incubation (Fig. 5), suggesting that the tested dust

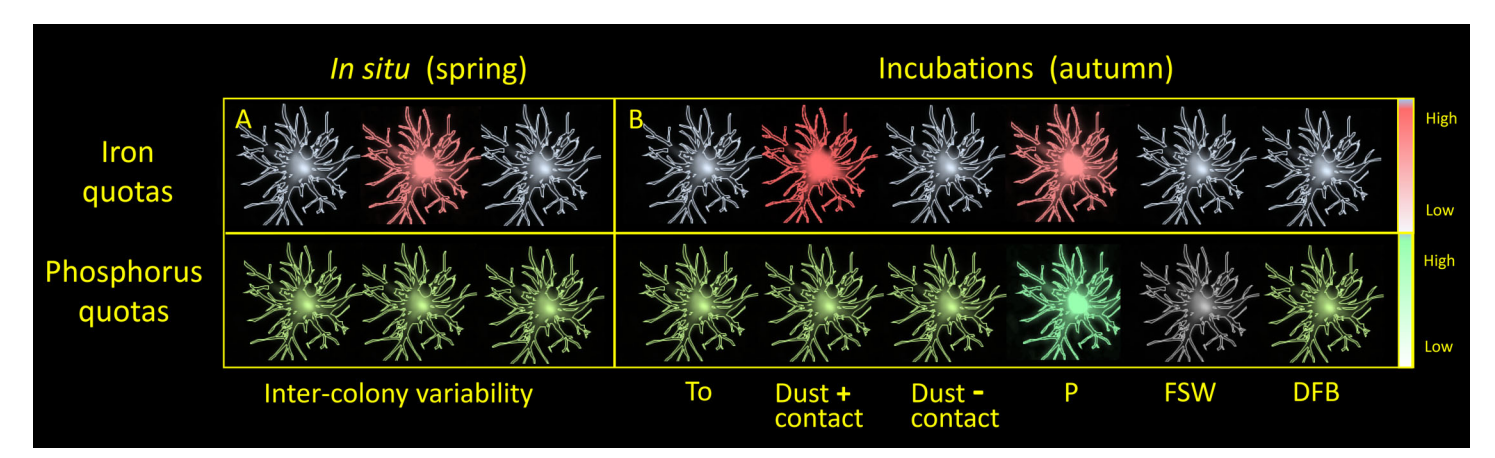


Fig. 7. Schematic summary of the distinct patterns of Fe and P quotas observed for in situ (a) and incubated (b) Red Sea *Trichodesmium* colonies. (a) Colonies collected over an entire season had homogeneous P quotas, but heterogeneous Fe quotas. (b) Phosphorus quotas responded rapidly to dissolved P addition or removal, but not to dust. Iron quotas remained unchanged when dust was present in a dialysis bag, but increased upon contact with dust, indicating active dissolution and uptake from dust. Dissolved Fe complexation with deferoxamine B (DFB) did not alter Fe quotas. P addition, in contrast, increased Fe quotas. Combined, our findings suggest that natural colonies obtain P from the dissolved phase, while Fe is acquired from the particulate phase, through contact-dependent active dissolution.

was not a good P source for Trichodesmium. This is not surprising, as Trichodesmium requires 10-100 times more P than Fe, while dust contains 10-100 times less P than Fe (Sañudo-Wilhelmy et al. 2001; Mackie et al. 2006; Anderson et al. 2010). Nonetheless, some of the dust-P is readily exchangeable (Stockdale et al. 2016), and P-related physiological responses to low-level dust addition have been reported in Atlantic or Red Sea natural colonies, including elevated N2-fixation rates and downregulation of the P-stress marker genes (Mills et al. 2004; Wang, et al. 2022a). Moreover, in a parallel study, similar dust incubations resulted in a decline in APA of single colonies, indicating alleviation of P-stress (Wang 2023). Considering the dust concentration (2 mg L^{-1}) , its P content $(70 \,\mu\text{mol P g}^{-1} \text{ dust; Stockdale et al. } 2016)$, and 10–20% solubility (Bonnet and Guieu 2004), we calculated a release of $\sim 10 \text{ nM PO}_4$ to the incubation bottle that contained 10–20 colonies. It is possible that the colonies acquired this P, but it was too low to detect, or that it was lost by binding to the container walls.

While dust did not impact P quotas, P-limitation, and/or addition of soluble P rapidly altered them (Fig. 5a). As indicated by the P-stress biomarker in our previous study (Wang, et al. 2022a), maintaining fresh colonies in FSW (with a background soluble P concentration of ~ 30 nM) gradually intensified P-limitation as the colony community grew, thereby potentially reducing the colonies' P quotas. Indeed, a drop in P quotas occurred within a day of incubation in FSW. Phosphorus quotas dropped further the next day, remaining constant and low in all other 7- to 8-d incubations. Incubated colonies had lower P quotas than in situ colonies, possibly reflecting seasonal variations in P-limitation between spring (in situ) colonies and autumn (incubated) colonies. Alternatively, the incubation process itself may have induced P-limitation. To further examine whether these quotas reflect P-

limitation, we compared the Fe/P ratios we obtained for single non-overlapping filaments with those of P-limited Atlantic colonies. Our values varied between 30 and 60 mmol Fe mol⁻¹ P and were comparable to those reported by (Nuester et al. 2012) and (Tovar-Sanchez et al. 2006) (Supporting Information Table S2). Additional studies also reported P-limitation of Red Sea colonies based on enzymatic activity and P-stress markers (Stihl et al. 2001; Mackey et al. 2007; Wang et al. 2022b).

Adding readily available P (10 µM PO₄) resulted in a rapid and significant increase in P quotas in most colonies (Fig. 5). Interestingly, P addition led to an apparent increase in Fe quotas in all incubations (Fig. 4). Since the incubated colonies were likely P-limited, these data may indicate that alleviation of P-limitation favors Fe uptake. The complex relationships between Fe and P uptake and various metabolic activities under Fe- and/or P-limitation and co-limitation have been intensively studied (Walworth et al. 2016; Tzubari et al. 2018; Held et al. 2020; Cerdan-Garcia et al. 2022). Fewer studies examined the impact of P (or Fe) limitation on the elemental stoichiometry of Trichodesmium (White et al. 2006; Nuester et al. 2012; Wang, et al. 2022b; Wang et al. 2024). However, we did not find research testing the impact of P addition (i.e., relieving P-limitation) on Fe uptake. A dedicated study is needed to examine whether P-limitation can impair Fe uptake and potentially induce Fe-limitation.

Spatial distribution within colonies

Comparing element distribution in the core and periphery of the colonies, we found that Fe, Mn, Ni, and P are core-enriched, As is core-depleted, and Ca is evenly distributed (Fig. 2; Supporting Information Table S3). In a previous study, we investigated the spatial distribution of Fe uptake from minerals (55 Ferrihydrite) by natural colonies (Basu et al. 2019). We

overlapped 2D 55Fe signals on colony images and observed a preferential 55Fe accumulation in the colony center. In the context of active mineral centering and dissolution by the colonies, we suggested that these patterns reflect the proximity of filaments to minerals, the accumulation of reactants (e.g., siderophores), and a reduced loss of dissolved Fe (Qiu et al. 2022; Eichner et al. 2023). Hence, the core enrichments of Fe and Mn, which are abundant in dust, align with our previous studies. Nonetheless, Ni and P, less abundant dust elements, were also core-enriched. Moreover, this pattern was observed in colonies from all treatments, including unmasked colonies (i.e., no dust identified) and those subjected to weeklong incubations in FSW (i.e., low particle load). These patterns, thus, probably reflect inherent colony features rather than localized nutrient "mining" from dust particles in the colony center.

The core enrichment of Fe, Mn, Ni, and P may result from differential allocation within each filament, but is more likely to reflect the presence of other microorganisms and organic matter. The amoebae-containing colonies provide a visual example of the effect of core-centered microorganisms on Ca and S distribution patterns (Fig. 2). Although we excluded the amoebae-containing colonies from the spatial analysis (Fig. 3). other microorganisms, such as bacteria and phytoplankton, may contribute to the elemental signal in the core. The physically complex colony core often contains secreted polysaccharides (and other macromolecules) that may retain cell debris, tiny particles, and bacteria (Steinberg et al. 2004; Bif et al. 2019; Kessler et al. 2020a, 2020b). Further research with higher-resolution synchrotron imaging is required to test whether elements are differentially allocated across the filaments.

Inter-colony variability in P and Fe quota

Substantial heterogeneity was reported for the large and complex *Trichodesmium* colonies in multiple measures, including metabolic rates, protein expression patterns, and interactions with particles (Eichner et al. 2017, 2019, 2020; Held et al. 2021; Wang, et al. 2022a; Shaked et al. 2023; Romanowicz et al. 2024). Indeed, single-colony APA measured in the same spring was also highly heterogeneous (Fig. 6c), likely reflecting the temporal dynamics of the rapidly changing activity of these enzymes. In contrast, the P quotas determined here were surprisingly homogeneous among in situ colonies from a specific morphotype and within the control (FSW) treatments (Fig. 6b). Elemental quotas result from the activity of many such enzymes over time and thus likely average out changes in nutrient supply and demand over the diurnal cycle and shorter time scales or over the colony's lifetime.

Iron quotas in the same treatments were more heterogeneous than the P quotas (Fig. 6). The higher heterogeneity in Fe quota may stem from variations in Fe nutrition in this dust- and particle-impacted environment, where dust particles in the water column represent hotspots of iron that occur in a

more concentrated but sporadic form, as compared to a dissolved nutrient that is more evenly distributed in the water column. In such an environment, Trichodesmium colonies likely impact Fe availability through dust solubilization, as shown in Fig. 4. Consequently, Fe nutrition may change according to the mineral-solubilizing microbiome composition et al. 2019; Koedooder et al. 2023) or physico-chemical conditions in the colony microenvironment (including pH and O2, which can both affect Fe availability to a limited extent Eichner et al. 2019). The homogeneity in P quotas, on the other hand, may reflect a more evenly distributed dissolved P source. This dissolved pool likely comprises a diverse array of inorganic and organic compounds, which Trichodesmium and associated bacteria access through multiple specialized pathways for phosphorus (P) acquisition (Orchard et al. 2010; Van Mooy et al. 2012; Frischkorn et al. 2018). These distinct nutritional modes can explain the frequent occurrence of large-scale and prolonged Trichodesmium blooms in coastal areas, which are rich in both suspended Fe particles and river-borne organic P compounds (Qi et al. 2023).

Summary

Applying a benchtop μ XRF, we examined the elemental composition of 106 natural *Trichodesmium* colonies collected from the dust-impacted Gulf of Aqaba and incubated for up to a week with dust and nutrients. Focusing on the Fe and P content of the colonies (i.e., quota), we identified distinct patterns that likely reflect the different sources of these nutrients (Figs. 4–7). Based on the in situ inter-colony variability and the changes in quotas during incubations, it appears that *Trichodesmium* obtains its Fe from dust (and particles), while P is sourced from the dissolved phase. The significance of dissolved P for phosphorus nutrition was evident from the rapid drop in P quotas during incubations in filtered seawater and the homogeneity in P quotas among in situ colonies. Furthermore, P quotas increased during incubations with added dissolved P but remained unchanged when incubated with dust.

The significance of dust (and particles) for the colonies' iron nutrition can be inferred from the lack of impact of DFB on Fe quotas, an established treatment for inducing Fe limitation by preventing dissolved Fe uptake. The ability to access Fe from particles may explain this observation. Compared to P quotas, in situ colonies had heterogeneous Fe quotas. We also observed a substantial, yet highly variable, increase in Fe quotas in incubations with dust. We thus postulate that this heterogeneity reflects the stochastic nature of dust as an iron source. Finally, colony-mineral interactions were identified as critical for Fe uptake from dust, as Fe quotas remained unchanged in incubations with dust in a dialysis bag. This novel finding of contact-dependent Fe uptake from dust aligns with multiple mechanistic studies documenting the role of *Trichodesmium* and associated microbes in dissolving insoluble

dust minerals, which may also explain the enrichment of the colony core with Fe. The ability of *Trichodesmium* to actively mine particles for Fe is of great ecological importance in particle-rich coastal water and dust-impacted open-ocean environments.

Author Contributions

Yeala Shaked, Meri Eichner, Ondrej Prášil, and Hendrik Küpper conceived the study and secured funding. Futing Zhang and Antonio Colussi planned and performed the experiments with substantial help from Siyuan Wang and Coco Koedooder and prepared the samples for analysis. Ana Mijovilovich performed the μ XRF measurements, analysis and instrument calibrations. Ana Mijovilovich, Antonio Colussi, Futing Zhang, and Yeala Shaked analyzed the data and prepared the figures and tables. Meri Eichner headed the culture-based calibration exercise, with Syed Nadeem Hussain Bokhari performing ICP measurements and instrument calibrations. Yeala Shaked wrote the manuscript, and everyone discussed the data and assisted in editing and revising the paper.

Acknowledgments

We thank Murielle Drey, Emanuel Sestieri, and Bojan Vujic for their assistance with field and experimental work and Benjamin Twining for valuable input on the data analysis. We thank the associate editor, Susanne Wilken, for insightful comments that improved this manuscript. We acknowledge multiple funding agencies for kind support through grants and scholarships including: Israel Science Foundation (260/11), Czech Academy of Sciences (RVO: 60077344), Ministry of Education, Youth and Sports of the Czech Republic with co-funding from the EU (project KOROLID CZ.02.1.01/0.0/ 0.0/15_003/0000336), Ministry of Education, Youth and Sports of the Czech Republic (project e-INFRA CZ LM2018140), GACR (24-11363S), ASSAMBLE+, Planning and Budgeting Committee (PBC) of the Council for Higher Education of Israel, and China Scholarship Council - Hebrew University of Jerusalem Scholarship Program.

Data Availability Statement

The data that support the findings of this study are available on request from the corresponding author. The data are not publicly available due to privacy or ethical restrictions.

References

- Anderson, L. D., K. L. Faul, and A. Paytan. 2010. "Phosphorus Associations in Aerosols: What Can They Tell Us About P Bioavailability." *Marine Chemistry* 120: 44–56. https://doi.org/10.1016/j.marchem.2009.04.008.
- Bar-Zeev, E., I. Avishay, K. D. Bidle, and I. Berman-Frank. 2013. "Programmed Cell Death in the Marine

- Cyanobacterium *Trichodesmium* Mediates Carbon and Nitrogen Export." *International Society for Microbial Ecology Journal* 7: 2340–2348. https://doi.org/10.1038/ismej. 2013.121.
- Basu, S., M. Gledhill, D. de Beer, S. G. Prabhu Matondkar, and Y. Shaked. 2019. "Colonies of Marine Cyanobacteria *Trichodesmium* Interact With Associated Bacteria to Acquire Iron From Dust." *Communications Biology* 2: 284. https://doi.org/10.1038/s42003-019-0534-z.
- Basu, S., and Y. Shaked. 2018. "Mineral Iron Utilization by Natural and Cultured *Trichodesmium* and Associated Bacteria." *Limnology and Oceanography* 63: 2307–2320. https://doi.org/10.1002/lno.10939.
- Benavides, M., J. Arístegui, N. S. R. Agawin, J. L. Cancio, and S. Hernández-León. 2013. "Enhancement of Nitrogen Fixation Rates by Unicellular Diazotrophs vs. *Trichodesmium* After a Dust Deposition Event in the Canary Islands." *Limnology and Oceanography* 58: 267–275. https://doi.org/10.4319/lo.2013.58.1.0267.
- Benavides, M., L. Conradt, S. Bonnet, et al. 2021. "Fine-Scale Sampling Unveils Diazotroph Patchiness in the South Pacific Ocean." *International Society for Microbial Ecology Communications* 1: 3. https://doi.org/10.1038/s43705-021-00006-2.
- Bergman, B., G. Sandh, S. Lin, J. Larsson, and E. J. Carpenter. 2013. "*Trichodesmium* A Widespread Marine Cyanobacterium With Unusual Nitrogen Fixation Properties." *Federation of European Microbiological Societies Microbiology Reviews* 37: 286–302. https://doi.org/10.1111/j.1574-6976.2012.00352.x.
- Berman-Frank, I., J. T. Cullen, Y. Shaked, R. M. Sherrell, and P. G. Falkowski. 2001. "Iron Availability, Cellular Iron Quotas, and Nitrogen Fixation in *Trichodesmium*." *Limnology and Oceanography* 46: 1249–1260. https://doi.org/10.4319/lo.2001.46.6.1249.
- Bif, M. B., M. S. de Souza, L. D. F. Costa, and J. S. Yunes. 2019. "Microplankton Community Composition Associated With Toxic *Trichodesmium* Aggregations in the Southwest Atlantic Ocean." *Frontiers in Marine Science* 6: 23. https://doi.org/10.3389/fmars.2019.00023.
- Boatman, T. G., G. J. G. Upton, T. Lawson, and R. J. Geider. 2020. "Projected Expansion of *Trichodesmium's* Geographical Distribution and Increase in Growth Potential in Response to Climate Change." *Global Change Biology* 26: 6445–6456. https://doi.org/10.1111/gcb.15324.
- Bonnet, S., M. Benavides, F. A. C. Le Moigne, et al. 2023. "Diazotrophs Are Overlooked Contributors to Carbon and Nitrogen Export to the Deep Ocean." *International Society for Microbial Ecology Journal* 17: 47–58. https://doi.org/10. 1038/s41396-022-01319-3.
- Bonnet, S., and C. Guieu. 2004. "Dissolution of Atmospheric Iron in Seawater." *Geophysical Research Letters* 31: 5–8. https://doi.org/10.1029/2003GL018423.

- Capone, D. G., J. P. Zehr, H. W. Paerl, B. Bergman, and E. J. Carpenter. 1997. "*Trichodesmium*, a Globally Significant Marine Cyanobacterium." *Science* 276, no. 5316: 1221–1229. https://doi.org/10.1126/science.276.5316.1221.
- Cerdan-Garcia, E., A. Baylay, D. Polyviou, et al. 2022. "Transcriptional Responses of *Trichodesmium* to Natural Inverse Gradients of Fe and P Availability." *International Society for Microbial Ecology Journal* 16: 1055–1064. https://doi.org/10.1038/s41396-021-01151-1.
- Chen, Y., A. Tovar-Sañchez, R. L. Siefert, S. A. Sanudo-Wilhelmy, and G. Zhuang. 2011. "Luxury Uptake of Aerosol Iron by *Trichodesmium* in the Western Tropical North Atlantic." *Geophysical Research Letters* 38. https://doi.org/10.1029/2011GL048972.
- Colussi, A., S. N. H. Bokhari, A. Mijovilovich, P. Koník, and H. Küpper. 2024. "Acclimation to Medium-Level Non-Lethal Iron Limitation: Adjustment of Electron Flow Around the PSII and Metalloprotein Expression in *Trichodesmium erythraeum* IMS101." *Biochimica et Biophysica Acta, Bioenergetics* 1865: 149015. https://doi.org/10.1016/j.bbabio.2023. 149015.
- Dyhrman, S. T. 2016. "Nutrients and their Acquisition: Phosphorus Physiology in Microalgae." In The Physiology of Microalgae, 155–183. Springer.
- Dyhrman, S. T., E. A. Webb, D. M. Anderson, J. W. Moffett, and J. B. Waterbury. 2002. "Cell-Specific Detection of Phosphorus Stress in *Trichodesmium* From the Western North Atlantic." *Limnology and Oceanography* 47, no. 6: 1832–1836. https://doi.org/10.4319/lo.2002.47.6. 1832.
- Eichner, M., S. Basu, M. Gledhill, D. De Beer, and Y. Shaked. 2019. "Hydrogen Dynamics in *Trichodesmium* Colonies and Their Potential Role in Mineral Iron Acquisition." *Frontiers in Microbiology* 10: 1565. https://doi.org/10.3389/fmicb. 2019.01565.
- Eichner, M., S. Basu, S. Wang, D. de Beer, and Y. Shaked. 2020. "Mineral Iron Dissolution in *Trichodesmium* Colonies: The Role of O_2 and pH Microenvironments." *Limnology and Oceanography* 65: 1149–1160. https://doi.org/10.1002/lno. 11377.
- Eichner, M., K. Inomura, J. J. Pierella Karlusich, and Y. Shaked. 2023. "Better Together? Lessons on Sociality from *Trichodesmium.*" *Trends in Microbiology* 31: 1072–1084. https://doi.org/10.1016/J.TIM.2023.05.001.
- Eichner, M. J., I. Klawonn, S. T. Wilson, et al. 2017. "Chemical Microenvironments and Single-Cell Carbon and Nitrogen Uptake in Field-Collected Colonies of *Trichodesmium* under Different pCO₂." *International Society for Microbial Ecology Journal* 11: 1305–1317. https://doi.org/10.1038/ismej.2017.15.
- Frischkorn, K. R., A. Krupke, C. Guieu, et al. 2018. "Trichodesmium Physiological Ecology and Phosphate Reduction in the Western Tropical South Pacific."

- *Biogeosciences* 15: 5761–5778. https://doi.org/10.5194/bg-15-5761-2018.
- Frischkorn, K. R., M. Rouco, B. A. S. Van Mooy, and S. T. Dyhrman. 2017. "Epibionts Dominate Metabolic Functional Potential of *Trichodesmium* Colonies From the Oligotrophic Ocean." *International Society for Microbial Ecology Journal* 11: 2090–2101. https://doi.org/10.1038/ismej. 2017.74.
- Gledhill, M., S. Basu, and Y. Shaked. 2019. "Metallophores Associated With *Trichodesmium erythraeum* Colonies From the Gulf of Aqaba." *Metallomics* 11: 1547–1557. https://doi.org/10.1039/c9mt00121b.
- Gralnick, J. A., and D. K. Newman. 2007. "Extracellular Respiration." *Molecular Microbiology* 65: 1–11. https://doi.org/10. 1111/J.1365-2958.2007.05778.X.
- Hansel, C. M., C. Buchwald, J. M. Diaz, et al. 2016. "Dynamics of Extracellular Superoxide Production by *Trichodesmium* Colonies From the Sargasso Sea." *Limnology and Oceanography* 61: 1188–1200. https://doi.org/10.1002/lno.10266.
- Held, N. A., K. M. Sutherland, E. A. Webb, et al. 2021. "Mechanisms and Heterogeneity of In Situ Mineral Processing by the Marine Nitrogen Fixer *Trichodesmium* Revealed by Single-Colony Metaproteomics." *International Society for Microbial Ecology Communications* 1: 35. https://doi.org/10.1038/s43705-021-00034-y.
- Held, N. A., E. A. Webb, M. M. McIlvin, et al. 2020. "Co-Occurrence of Fe and P Stress in Natural Populations of the Marine Diazotroph *Trichodesmium.*" *Biogeosciences* 17: 2537–2551. https://doi.org/10.5194/bg-17-2537-2020.
- Jiang, H. B., F.-X. Fu, S. Rivero-Calle, et al. 2018. "Ocean Warming Alleviates Iron Limitation of Marine Nitrogen Fixation." *Nature Climate Change* 8: 709–712. https://doi.org/ 10.1038/s41558-018-0216-8.
- Kessler, N., R. Armoza-Zvuloni, S. Wang, et al. 2020a. "Selective Collection of Iron-Rich Dust Particles by Natural *Trichodesmium* Colonies." *International Society for Microbial Ecology Journal* 14, no. 1: 91–103. https://doi.org/10.1038/s41396-019-0505-x.
- Kessler, N., S. M. Kraemer, Y. Shaked, and W. D. C. Schenkeveld. 2020b. "Investigation of Siderophore-Promoted and Reductive Dissolution of Dust in Marine Microenvironments Such as *Trichodesmium* Colonies." *Frontiers in Marine Science* 7: 45. https://doi.org/10.3389/fmars. 2020.00045.
- Koedooder, C., E. Landou, F. Zhang, et al. 2022. "Metagenomes of Red Sea Subpopulations Challenge the Use of Marker Genes and Morphology to Assess *Trichodesmium* Diversity." *Frontiers in Microbiology* 13: 879970. https://doi.org/10.3389/FMICB.2022.879970.
- Koedooder, C., F. Zhang, S. Wang, et al. 2023. "Taxonomic Distribution of Metabolic Functions in Bacteria Associated with *Trichodesmium* Consortia." *Msystems* 8: e0074223. https://doi.org/10.1128/msystems.00742-23.

- Kranzler, C., N. Kessler, N. Keren, and Y. Shaked. 2016. "Enhanced Ferrihydrite Dissolution by a Unicellular, Planktonic Cyanobacterium: A Biological Contribution to Particulate Iron Bioavailability." *Environmental Microbiology* 18: 5101–5111. https://doi.org/10.1111/1462-2920. 13496.
- Küpper, H., I. Šetlík, S. Seibert, et al. 2008. "Iron Limitation in the Marine Cyanobacterium *Trichodesmium* Reveals New Insights into Regulation of Photosynthesis and Nitrogen Fixation." *New Phytologist* 179: 784–798. https://doi.org/10. 1111/j.1469-8137.2008.02497.x.
- Langlois, R. J., M. M. Mills, C. Ridame, P. Croot, and J. LaRoche. 2012. "Diazotrophic Bacteria Respond to Saharan Dust Additions." *Marine Ecology Progress Series* 470: 1–14. https://doi.org/10.3354/meps10109.
- Lenes, J. M., B. A. Darrow, J. J. Walsh, et al. 2008. "Saharan Dust and Phosphatic Fidelity: A Three-Dimensional Biogeochemical Model of *Trichodesmium* as a Nutrient Source for Red Tides on the West Florida Shelf." *Continental Shelf Research* 28: 1091–1115. https://doi.org/10.1016/j.csr.2008.02.009.
- Lis, H., and Y. Shaked. 2009. "Probing the Bioavailability of Organically Bound Iron: A Case Study in the *Synechococcus*-Rich Waters of the Gulf of Aqaba." *Aquatic Microbial Ecology* 56: 241–253. https://doi.org/10.3354/ame01347.
- Luo, Y. W., S. C. Doney, L. A. Anderson, et al. 2012. "Database of Diazotrophs in Global Ocean: Abundance, Biomass and Nitrogen Fixation Rates." *Earth System Science Data* 4: 47–73. https://doi.org/10.5194/essd-4-47-2012.
- Mackey, K. R. M., R. G. Labiosa, M. Calhoun, J. H. Street, A. F. Post, and A. Paytan. 2007. "Phosphorus Availability, Phytoplankton Community Dynamics, and Taxon-Specific Phosphorus Status in the Gulf of Aqaba, Red Sea." *Limnology and Oceanography* 52: 873–885. https://doi.org/10.4319/lo.2007. 52.2.0873.
- Mackie, D. S., J. M. Peat, G. H. McTainsh, P. W. Boyd, and K. A. Hunter. 2006. "Soil Abrasion and Eolian Dust Production: Implications for Iron Partitioning and Solubility." *Geochemistry, Geophysics, Geosystems* 7. https://doi.org/10.1029/ 2006gc001404.
- McCarthy, J. J., and E. J. Carpenter. 1979. "Oscillatoria (Trsichodesmium) Thiebautii (Cyanophyta) in the Central North Atlantic Ocean." Journal of Phycology 15: 75–82. https://doi.org/10.1111/j.0022-3646.1979.00075.x.
- Mijovilovich, A., F. Morina, S. N. Bokhari, T. Wolff, H. Küpper, and H. Küpper. 2020. "Analysis of Trace Metal Distribution in Plants With Lab-Based Microscopic X-Ray Fluorescence Imaging." *Plant Methods* 16: 82. https://doi.org/10. 1186/s13007-020-00621-5.
- Mills, M. M., C. Ridame, M. Davey, J. La Roche, and R. J. Geider. 2004. "Iron and Phosphorus Co-Limit Nitrogen Fixation in the Eastern Tropical North Atlantic." *Nature* 429: 292–294. https://doi.org/10.1038/nature02550.
- Nuester, J., M. Newville, and B. S. Twining. 2014. "Distributions of Iron, Phosphorus and Sulfur Along Trichomes of

- the Cyanobacteria *Trichodesmium.*" *Metallomics* 6: 1141–1149. https://doi.org/10.1039/c4mt00042k.
- Nuester, J., S. Vogt, M. Newville, A. B. Kustka, and B. S. Twining. 2012. "The Unique Biogeochemical Signature of the Marine Diazotroph *Trichodesmium*." *Frontiers in Microbiology* 3: 1–15. https://doi.org/10.3389/fmicb.2012.00150.
- O'Neil, J. M. 1998. "The Colonial Cyanobacterium *Trichodesmium* as a Physical and Nutritional Substrate for the Harpacticoid Copepod *Macrosetella Gracilis.*" *Journal of Plankton Research* 20: 43–59. https://doi.org/10.1093/plankt/20.1.43.
- Orchard, E. D., J. W. Ammerman, M. W. Lomas, and S. T. Dyhrman. 2010. "Dissolved Inorganic and Organic Phosphorus Uptake in *Trichodesmium* and the Microbial Community: The Importance of Phosphorus Ester in the Sargasso Sea." *Limnology and Oceanography* 55, no. 3: 1390–1399. https://doi.org/10.4319/lo.2010.55.3.1390.
- Pabortsava, K., R. S. Lampitt, J. Benson, et al. 2017. "Carbon Sequestration in the Deep Atlantic Enhanced by Saharan Dust." *Nature Geoscience* 10: 189–194. https://doi.org/10.1038/ngeo2899.
- Paerl, H. W., L. E. Prufert-Bebout, and C. Guo. 1994. "Iron-Stimulated N2 Fixation and Growth in Natural and Cultured Populations of the Planktonic Marine Cyanbacteria *Trichodesmium* Spp." *Applied and Environmental Microbiology* 60: 1044–1047. https://doi.org/10.1128/aem.60.3.1044-1047.1994.
- Pierella Karlusich, J. J., E. Pelletier, F. Lombard, et al. 2021. "Global Distribution Patterns of Marine Nitrogen-Fixers by Imaging and Molecular Methods." *Nature Communications* 12, no. 1: 4160. https://doi.org/10.1038/s41467-021-24299-y.
- Polyviou, D., A. J. Baylay, A. Hitchcock, J. Robidart, C. M. Moore, and T. S. Bibby. 2018. "Desert Dust as a Source of Iron to the Globally Important Diazotroph *Trichodesmium*." *Frontiers in Microbiology* 8: 2683. https://doi.org/10.3389/fmicb.2017.02683.
- Qi, L., M. Wang, C. Hu, et al. 2023. "*Trichodesmium* Around Australia: A View From Space." *Geophysical Research Letters* 50: e2023GL104092. https://doi.org/10.1029/2023GL104092.
- Qiu, G. W., C. Koedooder, B. S. Qiu, Y. Shaked, and N. Keren. 2022. "Iron Transport in Cyanobacteria From Molecules to Communities." *Trends in Microbiology* 30: 229–240. https://doi.org/10.1016/j.tim.2021.06.001.
- Romanowicz, K. J., F. Zhang, S. Wang, et al. 2024. "Single-Colony MALDI Mass Spectrometry Imaging Reveals Spatial Differences in Metabolite Abundance Between Natural and Cultured Trichodesmium Morphotypes." *mSystems* 9: e01152-24. https://doi.org/10.1128/msystems.01152-24.
- Rubin, M., I. Berman-Frank, and Y. Shaked. 2011. "Dust- and Mineral-Iron Utilization by the Marine Dinitrogen-Fixer *Trichodesmium.*" *Nature Geoscience* 4: 529–534. https://doi.org/10.1038/ngeo1181.

- Sañudo-Wilhelmy, S. A., A. B. Kustka, C. J. Gobler, et al. 2001. "Phosphorus Limitation of Nitrogen Fixation by *Trichodesmium* in the Central Atlantic Ocean." *Nature* 411: 66–69. https://doi.org/10.1038/35075041.
- Shaked, Y., D. de Beer, S. Wang, et al. 2023. "Co-Acquisition of Mineral-Bound Iron and Phosphorus by Natural *Trichodesmium* Colonies." *Limnology and Oceanography* 68: 1064–1077. https://doi.org/10.1002/LNO.123292023.
- Shaked, Y., B. S. Twining, T. J. Browning, C. Koedooder, and C. F. Kranzler. 2024. "Trace Metal Biogeochemistry in the Ocean: From Chemical Principles to Biological Complexity." In Reference Module in Earth Systems and Environmental Sciences. Elsevier.
- Shaked, Y., Y. Xu, K. Leblanc, et al. 2006. "Zinc Availability and Alkaline Phosphatase Activity in *Emiliania huxleyi*: Implications for Zn-P Co-Limitation in the Ocean." *Limnology and Oceanography* 51: 299–309. https://doi.org/10.4319/lo.2006.51.1.0299.
- Sheridan, C. C., D. K. Steinberg, and G. W. Kling. 2002. "The Microbial and Metazoan Community Associated with Colonies of *Trichodesmium* Spp.: A Quantitative Survey." *Journal of Plankton Research* 24: 913–922. https://doi.org/10.1093/plankt/24.9.913.
- Sommer, U., E. Charalampous, S. Genitsaris, and M. Moustaka-Gouni. 2017. "Benefits, Costs and Taxonomic Distribution of Marine Phytoplankton Body Size." *Journal of Plankton Research* 39: 494–508. https://doi.org/10.1093/plankt/fbw071.
- Steinberg, D. K., N. B. Nelson, C. A. Carlson, and A. C. Prusak. 2004. "Production of Chromophoric Dissolved Organic Matter (CDOM) in the Open Ocean by Zooplankton and the Colonial Cyanobacterium *Trichodesmium* Spp." *Marine Ecology Progress Series* 267: 45–56. https://doi.org/10.3354/meps267045.
- Stihl, A., U. Sommer, and A. F. Post. 2001. "Alkaline Phosphatase Activities among Populations of the Colony-Forming Diazotrophic Cyanobacterium *Trichodesmium* Spp. (Cyanobacteria) in the Red Sea." *Journal of Phycology* 37: 310–317. https://doi.org/10.1046/j.1529-8817.2001. 037002310.x.
- Stockdale, A., M. D. Krom, R. J. Mortimer, et al. 2016. "Understanding the Nature of Atmospheric Acid Processing of Mineral Dusts in Supplying Bioavailable Phosphorus to the Oceans." *Proceedings of the National Academy of Sciences of the United States of America* 113: 14639–14644. https://doi.org/10.1073/pnas.1608136113.
- Tang, W., and N. Cassar. 2019. "Data-Driven Modeling of the Distribution of Diazotrophs in the Global Ocean." *Geophysical Research Letters* 46: 12258–12269. https://doi.org/10.1029/2019GL084376.
- Tang, W., E. Cerdán-García, H. Berthelot, et al. 2020. "New Insights into the Distributions of Nitrogen Fixation and Diazotrophs Revealed by High-Resolution Sensing and Sampling Methods." *International Society for Microbial Ecology Journal* 14: 2514–2526. https://doi.org/10.1038/s41396-020-0703-6.

- Torfstein, A., N. Teutsch, O. Tirosh, et al. 2017. "Chemical Characterization of Atmospheric Dust From a Weekly Time Series in the North Red Sea Between 2006 and 2010." *Geochimica et Cosmochimica Acta* 211: 373–393. https://doi.org/10.1016/j.gca.2017.06.007.
- Tovar-Sanchez, A., S. A. Sañudo-Wilhelmy, A. B. Kustka, et al. 2006. "Effects of Dust Deposition and River Discharges on Trace Metal Composition of *Trichodesmium* Spp. in the Tropical and Subtropical North Atlantic Ocean." *Limnology and Oceanography* 51: 1755–1761. https://doi.org/10.4319/lo.2006.51.4.1755.
- Tzubari, Y., L. Magnezi, A. Be'Er, and I. Berman-Frank. 2018. "Iron and Phosphorus Deprivation Induce Sociality in the Marine Bloom-Forming Cyanobacterium *Trichodesmium*." *International Society for Microbial Ecology Journal* 12: 1682–1693. https://doi.org/10.1038/s41396-018-0073-5.
- van der Ent, A., W. J. Przybyłowicz, M. D. de Jonge, et al. 2018. "X-Ray Elemental Mapping Techniques for Elucidating the Ecophysiology of Hyperaccumulator Plants." *New Phytologist* 218: 432–452. https://doi.org/10.1111/nph. 14810.
- Van Mooy, B. A., L. R. Hmelo, L. E. Sofen, et al. 2012. "Quorum Sensing Control of Phosphorus Acquisition in *Trichodesmium* Consortia." *International Society for Microbial Ecology Journal* 6: 422–429. https://doi.org/10.1038/ismej.2011.115.
- Visser, A. N., F. Zhang, L. Guttman, et al. 2025. "Unveiling the P-Solubilizing Potential of Bacteria Enriched from Natural Colonies of Red Sea *Trichodesmium* Spp." *Science of the Total Environment* 963: 178446. https://doi.org/10.1016/j.scitotenv.2025.178446.
- Walworth, N. G., F. X. Fu, M. D. Lee, et al. 2018. "Nutrient-Colimited *Trichodesmium* as a Nitrogen Source or Sink in a Future Ocean." *Applied and Environmental Microbiology* 84: e02137-17. https://doi.org/10.1128/AEM.02137-17.
- Walworth, N. G., F. X. Fu, E. A. Webb, et al. 2016. "Mechanisms of Increased *Trichodesmium* Fitness under Iron and Phosphorus colimitation in the Present and Future Ocean." *Nature Communications* 7: 12081. https://doi.org/10.1038/ncomms12081.
- Wang, S. 2023. Iron and Phosphorus Utilization from Dust by Natural Trichodesmium Colonies in the Gulf of Aqaba. Hebrew University.
- Wang, S., C. Koedooder, F. Zhang, et al. 2022a. "Colonies of the Marine Cyanobacterium *Trichodesmium* Optimize Dust Utilization by Selective Collection and Retention of Nutrient-Rich Particles." *IScience* 25. https://doi.org/10. 1016/j.isci.2021.103587.
- Wang, X., T. J. Browning, E. P. Achterberg, and M. Gledhill. 2022b. "Phosphorus Limitation Enhances Diazotroph Zinc Quotas." *Frontiers in Microbiology* 13: 853519. https://doi.org/10.3389/fmicb.2022.853519.
- Wang, X., T. J. Browning, E. P. Achterberg, and M. Gledhill. 2024. "Different Elemental Stoichiometries of Fe-Limited *Trichodesmium* when Grown under Inorganic and Organic

- Phosphorus Sources." *Limnology and Oceanography* 69: 2881–2895. https://doi.org/10.1002/LNO.12716.
- Webb, E. A., R. W. Jakuba, J. W. Moffett, and S. T. Dyhrman. 2007. "Molecular Assessment of Phosphorus and Iron Physiology in *Trichodesmium* Populations from the Western Central and Western South Atlantic." *Limnology and Oceanography* 52: 2221–2232. https://doi.org/10.4319/lo.2007.52. 5.2221.
- White, A. E., Y. H. Spitz, D. M. Karl, and R. M. Letelier. 2006. "Flexible Elemental Stoichiometry in *Trichodesmium* Spp. and Its Ecological Implications." *Limnology and Oceanogra-phy* 51: 1777–1790. https://doi.org/10.4319/lo.2006.51.4. 1777.

Zhang, F., S. Wang, A.-N. Visser, et al. 2024. "Recurrent Association Between *Trichodesmium* Colonies and Calcifying Amoebae." *International Society for Microbial Ecology Communications* 4: ycae137. https://doi.org/10.1093/ismeco/ycae137.

Supporting Information

Additional Supporting Information may be found in the online version of this article.

Submitted 26 January 2025 Revised 20 June 2025 Accepted 17 August 2025